

Weakening mechanism and energy budget of laboratory earthquakes

*Alexandre Schubnel¹, François Passelègue², Nicolas Brantut³, Soumaya Latour⁶, Harsha Bhat⁴, Stefan Nielsen⁵, Raul Madariaga¹

1.Laboratoire de géologie, Ecole Normale Supérieure, Paris, France, 2.University of Manchester, UK, 3.University College London, UK, 4.IPGP, France, 5.Durham University, France, 6.IRAP, Toulouse, France

The dynamics of earthquake ruptures in subduction zone are expected to be partially governed by the dehydration of minerals during shear heating. In this study, we conducted and compared results coming from stick-slip experiments on Westerly granite, serpentized peridotite, and serpentinite. Experiments were conducted under triaxial loading at confining pressures of 50 and 100 MPa. The angle between the fault plane and the maximum stress was imposed to be equal to 30 degrees. Using a dual gain system, a high frequency acoustic monitoring array recorded particle acceleration during macroscopic stick-slip events and premonitory background microseismicity. In addition, we used an amplified strain gage located at 3 mm to fault plane to record the dynamic stress change during laboratory earthquakes. In all rocks, we show that increasing the stress acting on the fault leads to an increase of the seismic slip, which in turn leads to a decrease in the dynamic friction coefficient. However, for a same initial stress, displacements are larger in serpentized peridotite and in serpentinite than in Westerly granite. While the partial melting of the fault surface is observed in each rock tested, the dynamic friction drop is larger in peridotite and serpentinite. This larger friction drop is explained by the dehydration of antigorite, which leaves a partially amorphised material and leads to the production of a low viscosity melt. Finally, using theoretical assumptions, we show that the radiation efficiency of laboratory earthquakes is larger in peridotite and serpentinite than in granite. This calculation is supported by larger elastic wave radiation, and by microstructural analysis.

Keywords: friction, dehydration, critical weakening distance

Revisiting the slip-weakening friction: probe into the true source properties from off-fault measurements

*Shiqing Xu¹, Eiichi Fukuyama¹, Futoshi Yamashita¹, Kazuo Mizoguchi², Shigeru Takizawa¹, Hironori Kawakata³

1.Nat'l Res. Inst. Earth Sci. Disas. Prev., 2.Centr. Res. Inst. Elect. Pow. Ind., 3.Ritsumeikan University

Slip-weakening friction, as evidenced by earlier pioneer rock fracture/friction experiments, has been widely used for numerically simulating earthquake ruptures, and for estimating earthquake source properties from seismological observations. Despite the great success, the accuracy of this constitutive relation is poorly known in the lab: measurements made close to the fault (yet still off the fault) were often assumed without validation to be the direct recordings of on-fault properties. Until recently, several works challenged this assumption, and showed that it may even lead to incorrect interpretation of rupture mode at speed close to the Rayleigh wave speed. This raises a concern on how to probe the true source properties on the fault using off-fault measurements, which was generally overlooked in the geophysical community.

To answer the question, we utilize a large-scale direct shear apparatus at NIED to monitor near-fault strain change during labquakes. By comparing our strain data with common slip-weakening model predications at various locations progressively away from the fault, we see systematically a decrease in apparent peak friction and an increase in apparent breakdown zone size. These features reflect the smearing out of the strain field away from the sharp rupture front. On the other hand, the initial strain before failure and the residual strain after the breakdown process are less sensitive to the sampling location, because the strain field is more homogeneous at those locations without sharp features. By fitting the strain data with templates created from a specific slip-weakening model, we are able to estimate the true source properties during labquakes within the framework of that model. If more data points were available, it would be even possible to probe the true "rupture distribution function" (Andrews, JGR 1976). In any case, our study suggests that care be taken when interpreting measurements during labquakes, especially when sharp features are involved during the rupture breakdown process (e.g. at a scale more than two times smaller than the source-recorder distance). Given the well-known Lorentz contraction effect, we may never be able to directly measure certain rupture properties at speed very close to the limit speed, which ultimately requires some indirect approaches.

Keywords: Slip-weakening friction, Dynamic rupture, Friction experiment

Understanding characteristics of granular convection by visualizing rotation of individual particles in tapped granular bed

*Noa Mitsui¹, Naoki Iikawa¹, Mahesh BANDI², Hiroaki Katsuragi¹

1.Graduate School of Environmental Studies, Nagoya University, 2.OIST

Granular material is defined by a collection of athermal particles, and it sometimes behaves like fluid despite solid property of each particle [1]. One of the fluid-like behaviors is convection of granular bed induced by vertical vibration, and it can be observed in laboratory experiments with various types of particles and vibrations. Recent studies propose that granular convection relates to resurfacing process of small asteroids covered with regolith (e.g., [2]). Thus the mechanism of the granular convection is not only physical but also geophysical problem.

One of the ways to understand the mechanism of granular convection is to monitor all degrees of freedom (DOF) of individual particles as well as to monitor the collective motion such as convection. The considered DOF of individual particles are (1) translational and (2) rotational velocities of each particle and (3) contact forces applied between particles besides body forces. However, in most of laboratory experiments, only translational velocities have been monitored (e.g., [3]). Recent study has visualized contact forces by using photoelastic discs [4,5]. However, they have not monitored rotational motion of particles. Particularly, although the particle rotation has not been measured well so far, it could significantly relate to the mechanism of granular convection.

In this study, we are going to monitor all these DOF in granular convection by using photoelastic discs. We use bidisperse photoelastic discs to make two-dimensional granular layer. Then, vertical intermittent tapping is applied to the granular layer by using an electromagnetic vibrator. We conducted experiments with several tapping conditions (duration and the maximum acceleration of tapping impulse). The photoelastic discs are painted with a fluorescent paint along the diameter to visualize the rotation by using ultraviolet-light illumination [6].

All DOF of individual particles in each tapping can be obtained as follows. Figure shows three types of pictures taken in this experiment. They are taken by using (a) white light source, (b) ultraviolet-light illumination, and (c) white light source under cross-polarized mode, respectively. Translational velocity and associated vorticity of granular convection are obtained by analyzing (a). The rotational velocities of individual particles are obtained by analyzing (b). In addition, the contact forces can be computed by (c). As the first step, we will focus on the analysis of (a) and (b) in this study, and understand the relation between granular convection and rotational velocities of individual particles.

[1] Jaeger, H. M., S. R. Nagel, and R. P. Behringer (1996) *Rev. Mod. Phys.*, 68, 1259-1273.

[2] Yamada, T., K. Ando, T. Morota, and H. Katsuragi (2015) arXiv: 1508.06485.

[3] Shukla, P., I.H. Ansari, R.M. van der Meer, D. Lohse, and M. Alam (2014) *J. Fluid Mech.*, 761, 123-167.

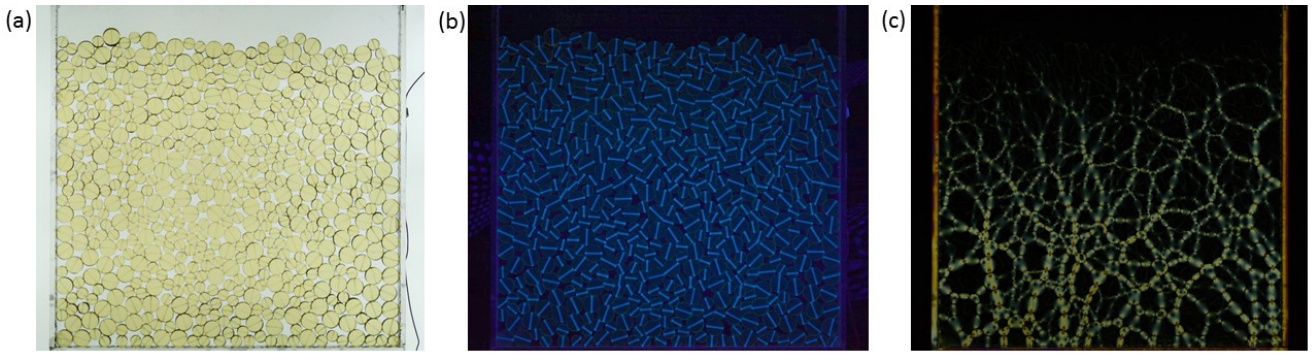
[4] Iikawa, N., M. M. Bandi, and H. Katsuragi (2015) *J. Phys. Soc. Jpn.* 84, 094401.

[5] Bandi, M. M., M. K. Rivera, F. Krzakala, and R. E. Ecke (2013) *Phys. Rev. E.*, 87, 042205.

[6] Puckett, J. G., and K. E. Daniels (2013) *Phys. Rev. Lett.* 110, 058001.

Figure. Samples of photos taken by using (a) white light source, (b) ultraviolet-light illumination, and (c) white light source under cross-polarized mode, respectively.

Keywords: granular matter, granular convection, rotation



Granular friction: Triggering slip motion with small vibrations

*Valerie Vidal¹, Henri Lastakowski¹, Jean-Christophe Géminard¹

1.Laboratoire de Physique, Ecole Normale Supérieure de Lyon - CNRS

We investigate experimentally the influence of mechanical vibrations on the characteristics of granular friction. The experimental system consists of a slider and a cantilever spring, pulled at constant velocity over a granular layer. The slider mass, spring stiffness and pulling velocity are chosen such that without mechanical perturbances, the slider exhibits a classical stick-slip motion. Horizontal vibrations are then applied to the whole system. When increasing either the amplitude or frequency of the vibrations, the amplitude of the stick-slip motion decreases, until the system exhibits a transition to a continuous slip motion. Previous numerical studies pointed out the acceleration of imposed vertical vibrations as the governing parameter for the transition, with a value of the order of the gravitational acceleration. In contrast to these results, we show that the quantity that controls the frictional properties is the characteristic velocity, and not the acceleration, of the imposed mechanical vibrations. The critical velocity at which the system undergoes the transition to a continuous slip motion is very small, of the order of 100 microns/s. Thus, when the system is statically loaded, the typical acceleration of the vibrations which trigger large slip events is much smaller than the gravitational acceleration. These results may be relevant to understand dynamic earthquake triggering by small ground perturbations.

Keywords: granular friction, stick-slip motion, vibrations, dynamic earthquake triggering

A new rheological model of magma for representing transition from flow to fracture

*Mie Ichihara¹

1. Earthquake Research Institute, University of Tokyo

Whether a flowing magma with increasing strain rate becomes brittle or ductile is an important but puzzling problem in considering eruption dynamics. The criterion of the brittle/ductile transition that is currently used in volcanology is thoroughly based on the linear viscoelastic model assuming small deformation. However, flow of magma to fracture is not in the linear regime, and the current model to describe the phenomenon reveals inconsistency. Here the problem is re-considered and a new constitutive equation for magma is proposed.

Magma rheology is frequently represented by the linear Maxwell model, which consists of a viscous element and an elastic element in line. It behaves elastically in a short time or in high-frequency oscillation, and viscously in a long time or in low-frequency oscillation. The dynamic viscosity is defined in oscillatory deformation as the amplitude ratio of the stress to the strain rate and is a function of frequency. For both of magma and the Maxwell model, the dynamic viscosity is constant in the low-frequency viscous regime, and decreases as frequency increases in the elastic regime. The frequency separating the viscous and elastic regimes is inversely proportional to the low-frequency limit of the dynamic viscosity.

There are two well-known rheological laws that generally hold for polymeric fluids including magma. The one is time-temperature superposition, which indicates that change of rheology with decreasing temperature is equivalent with increasing frequency. The other is what is called Cox and Merz rule: the steady-state viscosity as a function of strain rate under continuous flow is the same as the dynamic viscosity as a function of frequency and it decreases with increasing strain rate.

Combining the two laws has led the idea that flowing magma may enter the glassy (elastic) regime either by cooling or increasing strain rate (Dingwell, 1996). This idea has significantly influenced modeling of volcanic phenomena. Although the viscosity increases with cooling, it decreases with increasing strain rate. It is not clear whether transition to the glassy state with decreasing viscosity by increasing strain rate is the same as that by cooling.

In the area of non-linear physics, on the other hand, the glassy state is regarded as the jammed state and the glassy to ductile transition is linked to yielding (Trappe et al., 2002). In this view, a material goes from a glassy state to flow with increasing strain rate, which is opposite to the concept in volcanology. Moreover, Miyazaki et al. (2006) shows that the dynamic viscosity in the oscillatory flow either decreases or increases as the strain rate amplitude increases depending on how it is increased, that is the product of the frequency and the strain amplitude is increased whether by increasing the frequency or by increasing the strain amplitude.

The linear Maxwell model does not represent the Cox and Merz rule or non-linear behavior in large deformation. Here a new phenomenological model is proposed, which consists of the Maxwell model with a viscous element having variable viscosity and an equation representing change of the viscosity by forcing and relaxation. It can represent the behavior similar to the Cox and Merz rule. Using the new model, it is shown that not the strain rate but the strain acceleration is essential for bringing the flow to the brittle regime.

Keywords: magma, flow and fracture, rheology, Volcanic eruption

High precision prediction of dynamic instabilities

*Tetsuo Yamaguchi¹

1. Graduate school of Engineering, Kyushu University

Prediction of dynamic instabilities in collapse of buildings, landslides and earthquakes is very important for preventing damages. Here we report our experiments on multiple degree-of-freedom snap-through buckling where we can predict the onset of dynamic instabilities with high precision. We also apply this idea to laboratory earthquake experiments and discuss how it works.

Keywords: buckling, earthquake, prediction, Critical slowing down

Earthquake model experiments in a viscoelastic fluid: A scaling of decreasing magnitudes of earthquakes with depth

*Atsuko Namiki¹, Tetsuo Yamaguchi², Ikuro Sumita³, Takehito Suzuki⁴, Satoshi Ide⁵

1.Graduate School of Integrated Arts and Sciences, Hiroshima University, 2.Department of Mechanical Engineering, School of Engineering, Kyushu University, 3.Graduate School of Natural Science and Technology, Kanazawa University, 4.Department of Physics and Mathematics, Aoyama Gakuin University, 5.Department of Earth and Planetary Science, University of Tokyo

We performed shear deformation experiments using quasi-Maxwell fluids. We found that, depending on the strain rates, the same material generates earthquakes associated with the elastic rebound and deforms viscously. Around the threshold, elastic rebound releases a certain fraction of the interseismic displacement, but the other fraction remains as a result of the viscous relaxation. We applied our experimental results to a subduction zone, in which the upper part of the hanging wall behaves as an elastic layer and generates seismicity, while the deeper part behaves as a viscous fluid and subducts with the slab. Our experimental results suggest that, around the boundary of the elastic and viscous layers, seismicity can occur, but only some part of the interseismic displacements is released. The experimentally obtained threshold of the seismic activity is determined by the combination of the subduction velocity v , the viscosity of the hanging wall η , the fault length W , and the adhesive stress σ , $v \eta / (W \sigma) > 1$. This threshold suggests that if the viscosity of the hanging wall decreases with depth, the maximum size of the earthquakes also decreases with depth, and, finally, seismicity disappears. This hypothesis is consistent with the observed fact that slow earthquakes, characterized by their small magnitudes, are observed at the downdip limit of the seismogenic zone.

Reference: Namiki, A., T. Yamaguchi, I. Sumita, T. Suzuki, and S. Ide (2014), Earthquake model experiments in a viscoelastic fluid: A scaling of decreasing magnitudes of earthquakes with depth, J. Geophys. Res. Solid Earth, 119, 3169–3181, doi:10.1002/2014JB011135.

Keywords: Viscous relaxation, Shear deformation, Maxwell fluid

Striation process at subduction zones of terrestrial planets

*Takao Eguchi¹

1.Dept. of Earth and Ocean Sciences, School of Applied Sciences, National Defense Academy

We consider the basic nature of dynamics at zonal convergence boundaries between separate lithospheres on the terrestrial planets.

In this study the surface of the terrestrial planet considered is covered with several spherical rigid lithospheres having non-negligible individual horizontal motions relative to the deeper planetary structure.

We can analyze the basic aspects of various features at lithosphere boundary zones using the classical concept of plate tectonics.

Smaller-scaled convex topography and/or irregular shallow structure of the underthrusting-side lithosphere at the contacting interface of the consuming boundaries would cause a sort of striation (or wear-related) process with the elastic and inelastic deformation.

The continuous striation process should record the direction of the relative lithosphere motions on the planer interface.

However, in the case of tightly coupled boundaries with the intermittent history of greater seismic events, the striation process may not be a steady state problem.

On the earth, a large number of marine surveys have been unveiling the detailed characteristics of both the topography and sub-surface structure of oceanic lithospheres around subduction zones. Recent studies of sophisticated multichannel seismic prospecting identified fine-scaled non-uniform topography of the plate-interface just beneath the fore-arc overriding lithosphere at the Japan trench and Nankai trough subduction zones, etc.

Using engineering methods and survey results, we can decode the details of the strain-rate dependent (seismic/aseismic) striation process on the lithospheric-interface with the local convex topography etc. at the terrestrial subduction zones.

For the striation process, we should incorporate the effect of both the spherical bending and subsequent buckling of the downgoing-side lithosphere with the age-dependent EET (effective elastic thickness).

Although the spherical buckling at the consuming boundary requests a specific geometry of surface curvature mainly depending on the EET, the past tectonic history including the deeper material flow regime etc. would also influence the three dimensional morphology of the downgoing lithosphere. Furthermore, the difference of the elastic constants between the overriding and underthrusting lithospheres may affect dynamically on the striation and on the other seismological phenomena. We then discuss mathematically the strain-rate dependent striation process using a simplified mechanical model for the larger inter-lithosphere seismic events.

Keywords: striation process, wear, inelastic deformation, spherical buckling, subduction zone

Measurements of elastic wave velocity of Aji granite during triaxial compression tests under pore pressure

*Kanta Zaima¹, Ikuo Katayama¹

1.Department of Earth and Planetary Systems Science, Hiroshima University

Elastic wave velocity is one of important physical properties to investigate structure in the Earth's interior. Because of a markedly change in elastic wave velocity at the presence of fluid, the geothermal fluid reservoir is frequently detected through seismic tomography. Previous laboratory experiments have carried to investigate effect of confining pressure (e.g. Nur and Simmons, 1969), axial stress during deformation (e.g. Gupta, 1973; Bonner, 1974; Lockner et al, 1977; Yukutake, 1989; Ayling et al. 1995), fluid saturation (e.g. Nur and Simmons, 1969). However, there are few studies examining elastic wave velocity change on fracture process under pore pressure. In this study, we examined change of elastic wave velocity, amplitude and wave period during triaxial compression tests under pore pressure as a fundamental research on estimating of artificial geothermal reservoir on hot dry rock system.

We used Aji granite with a cylindrical shape, 40 mm long and 20 mm in diameter. For triaxial compression tests, we used intra-vessel deformation and fluid flow apparatus at Hiroshima University and deformed sample at 0.01 mm/min displacement rate. On dry condition, confining pressure was 20 MPa, and on wet condition, we used water as a pore fluid and confining pressure was 20MPa and pore pressure was 10 MPa. We kept pore pressure constant using syringe pump and calculated approximate porosity from volume change of fluid at syringe pump. We adopted pulse transmission method using electric transducers directly attached on the sample, and elastic wave velocity (V_p , V_s), amplitude and wave period from waveforms were recorded by oscilloscope.

We observed a systematic change of elastic wave velocity possibly due to closure, growth and formation of cracks during triaxial deformation. While elastic wave velocity was increased due to closure of preexisting cracks at the primary stage of deformation, it decreased markedly at the late stage of deformation. V_p/V_s tends to increase in association with development of deformation on wet condition while it decreases on dry condition. These data are consistent with theoretical model by O'Connell and Budiansky (1974), in which fluid filled cracks increase V_p/V_s but open (dry) cracks have an opposite influence. Based on the model of O'Connell and Budiansky (1974), crack density is suppressed during deformation under wet experiments. During triaxial deformation amplitude was attenuated and wave period became long as a consequence of increasing cracks in the specimens. Attenuation of P wave is relatively small on wet condition because of less scattering of elastic wave at crack surfaces with water. On the other hand, amplitude of S wave vibrated perpendicular to compressional axis tends to increase at initial of deformation, because S wave is sensitive to closure of horizontal cracks. Our experimental results show a correlation between porosity and elastic wave velocity, and we could use this relation to infer extent of fluid reservoir through seismic wave velocity.

Keywords: elastic wave velocity, triaxial deformation, crack density, pore pressure

Role of super critical fluids in quasi-static fracture process of earthquake nucleation
-case of 1965-1967 Matsushiro earthquake swarm-

*Yuji Enomoto¹, Tsuneaki Yamabe², Nobuo Okumura³

1.Shinshu Univeristy, Department of Textile Engineering, Fii, 2.Shinshu University, Department of Textile Engineering, 3.Genesis Research Institute, Inc.

None

Keywords: Fracture, Super critical fluids, Fractoemisson

Estimating stress field from seismic moment tensor data based on the flow rule in plasticity theory

*Satoshi Matsumoto¹

1. Institute of Seismology and Volcanology, Faculty of Sciences, Kyushu University

Stress field is a key factor controlling earthquake occurrence and crustal evolution. A method that slip data on many pre-existing faults reveals relative stress tensor in a region have been applied many regions. On the other hand difficulty of the method arises due to non-linear relation of slip vector to traction on a fault.

Here, we show stress field in a region with seismic activity can be estimated from sum of seismic moment tensors in the region based on classical equation in plasticity theory. Seismic activity is a phenomenon relaxing crustal stress and creates inelastic deformation in a medium due to faulting, which suggests the medium could behave as plastic body. The simple mathematical manipulation make easy to estimate stress field in a region and to develop inversion method in further studies.

Keywords: seismic moment tensor, stress field

Stress states in the deep part of subduction megathrust estimated from dynamically recrystallized grain size and dislocation creep flow laws of quartz

*Ichiko Shimizu¹, Tadamasa Ueda¹

1.Department of Earth and Planetary Science, Graduate School of Science, University of Tokyo

Strength of the continental lithosphere has been extensively studied, but little is known about stress states in subduction zone megathrusts. In this paper, we estimate paleo-stress in a Cretaceous subduction zone of the Sanbagawa belt in southwest Japan, using grain size piezometers and dislocation creep flow laws of quartz.

Laboratory studies showed that recrystallized grain size in dislocation creep is primarily controlled by the applied stress but physical basis of the piezometric relations is still in debate. Theoretical models predict that the steady-state grain size in dynamic recrystallization (DRX) is not only dependent on stress, but also on temperature. The common idea among existing theories is that competition between grain-boundary formation, and grain growth determines the steady-state grain size. For grain growth, grain boundary migration driven by strain-energy (ρ GBM), or that driven by surface-energy (γ GBM), have been considered. Both processes result in overall coarsening, but in the case of ρ GBM, strain-free small grains grow with the expense of larger deformed grains, while in γ GBM, small grains shrink and larger grains grow. A simple nucleation-and-growth model with ρ GBM produces a left-skewed distribution on a section that is approximated by a log-normal distribution with a single scaling parameter, d_c (Shimizu, 1999). In addition to subgrain rotation (SGR) nucleation and grain growth by ρ GBM, surface-energy drags were also taken into account in the revised theoretical piezometer (Shimizu, 2012).

We analyzed microstructures of quartz schists (meta-chert) taken from the Asemi-gawa root, central Shikoku. The grain size of quartz was measured by tracing grain boundaries on microphotographs and by mapping crystallographic orientations using the electron back-scattered diffraction (EBSD) method (Ueda & Shimizu, 2016, JpGU). Observed grain size distributions (GSDs), which were characterized by increasing numbers with decreasing grain size, were far different from bell-shaped distributions known for static grain growth driven by surface energy, and more like the theoretical distribution derived for the nucleation-and- ρ GBM model.

To estimate differential stress, we applied the revised theoretical piezometer (Shimizu, 2012) assuming that the grain size at the largest volume fraction corresponds to d_c . The paleo-stress estimates were also done by extrapolating dislocation flow law of wet quartz to the peak metamorphic temperatures. Preliminary results obtained for the sample in the garnet zone (ca. 500 °C) were within reasonable agreement with the dislocation creep model, whereas direct application of the experimental piezometer proposed by Stipp and Tullis (2003), re-calibrated by Holyoke & Kronenberg (2010), gives considerably smaller estimates.

References

- Holyoke, C.W. and Kronenberg, A.K. (2010). *Tectonophysics*, 494, 17-31.
 Shimizu, I. (1999). *Philosophical Magazine A*, 79, 1217-1231.
 Shimizu, I. (2012) In: "Recrystallization", edited by Krzysztof Sztwiertnia, InTech, ISBN 978-953-51-0122-2, pp. 371-386.
 Stipp, I. and Tullis, J. (2003). *Geophys. Res. Lett.*, 30, 2088-2092.

Keywords: differential stress, dynamic recrystallization, dislocation creep, grain size distribution, quartz, Sanbagawa metamorphic belt

Experimental evaluation of grain-size-sensitive creep and grain-size-insensitive creep of quartz

*Jun-ichi Fukuda¹, Caleb W. Holyoke², Andreas K. Kronenberg¹

1.Department of Geology and Geophysics, Texas A&M University, 2.Department of Geosciences, University of Akron

Plastic deformation of polycrystalline materials is categorized into two main mechanisms; one controlled by grain boundary process which depends on grain size (grain-size-sensitive creep; GSS creep) and the other controlled by intragrain dislocation process which does not depend on grain size (grain-size-insensitive creep; GSI creep). Studies of experimentally deformed and naturally deformed rocks suggest that in general, the transition between GSS and GSI creep can occur in the grain size of the micrometer order.

Quartz controls the ductile strength of continental rocks because of its abundant existence and weakness. Therefore, a lot of experimental studies have been done to construct the flow laws of quartz ductile deformation. Most experiments used large grain aggregates such as a few hundred μm of each grain, which promote GSI (dislocation) creep. The stress exponents were 3-4 and the microstructures exhibit elongated grains and/or recrystallized grains with host large grains. The host grains still constitute the large volume of the aggregates, leading to GSI creep. The mechanical properties of GSS creep are not well known. In this study, we use fine-grained quartz to experimentally demonstrate GSS creep and its transition to GSI creep.

We hot pressed fine-grained quartz powder of $\sim 2 \mu\text{m}$ in a solid-pressure-medium deformation (Griggs-type) apparatus at 1.5 GPa and 900°C . We observed systematic grain growth from $2 \mu\text{m}$ to $25 \mu\text{m}$ with increasing annealing times from 1 hour to 240 hours. The hot-pressed samples show polygonal grain shapes, tight grain boundaries, and no lattice preferred crystallographic orientations (LPOs). Next, strain-rate stepping experiments were performed under 1.5 GPa, $900\text{-}600^\circ\text{C}$, and the strain rates of $10^{-3.5}\text{-}10^{-6.0}/\text{sec}$. At 900 and 800°C , the stress exponents determined were $n=1.5\text{-}2.0$ (av. 1.7) regardless of the different hot press durations. At temperatures down to 600°C , the stress exponents increased up to 5. The microstructure of the samples shows undulatory extinction and recrystallized fine grains of $1 \mu\text{m}$. The crystallographic orientations have weak LPOs that reflect some crystal plasticity and recrystallization. The later stage of deformation appears to be controlled mostly by GSS creep of finely recrystallized grains, as indicated by low stress exponents. Temperature stepping experiments show corresponding two trends; one at $900\text{-}750^\circ\text{C}$ and the other at $700\text{-}550^\circ\text{C}$. The activation energies for the high temperature data were $160\text{-}200 \text{ kJ/mol}$ (av. 180 kJ/mol) with the stress exponents of 1.7. The strength changes by pressure stepping corresponded to the water fugacity changes. The obtained water exponent is $r=1$ with $n=1.7$.

We extrapolate our GSS creep data to natural conditions together with previous flow laws for quartz dislocation creep. Under mid-crustal conditions where the temperature and strain rate conditions are around 400°C and $10^{-14}/\text{sec}$, respectively, the transition from dislocation creep to GSS creep is predicted at a grain size of $\sim 10 \mu\text{m}$. This result is consistent with observations for natural quartz deformed by GSS creep. Our data indicate that the transition from dislocation creep to GSS creep occurs at crustal conditions for fine-grained quartz-rich rocks.

Keywords: Quartz rheology, Flow law, Crustal strength, Griggs-type deformation apparatus

Rheological weakening due to phase mixing of olivine + orthopyroxene aggregates

*Miki Tasaka^{1,2}, Mark E Zimmerman², David L Kohlstedt²

1.Niigata University, 2.University of Minnesota

To understand the processes involved in rheological weakening due to phase mixing in olivine + orthopyroxene aggregates, we have conducted high-strain torsion experiments on samples of iron-rich olivine + orthopyroxene. Samples with volume fractions of pyroxene, $f_{px} = 0.3$, were deformed at a temperature of 1200°C and a confining pressure of 300 MPa using a gas-medium apparatus to total shear strains up to $\gamma \approx 26$.

Values for the stress exponent of $n \approx 3$ and grain size exponent of $p \approx 1$ at lower strain ($1.9 \leq \gamma \leq 4.2$) and $n \approx 2$ and $p \approx 3.5$ at higher strain ($\gamma \geq 24$) were determined from a linear least-squares fit to the strain rate, stress, and grain size data using a power-law creep equation. These values of n and p indicate that our samples deformed by dislocation-accommodated grain boundary sliding at lower strain, with an increased contribution of diffusion creep at higher strain.

The microstructures observed in samples deformed to lower strain are consistent with structures induced by a dislocation-accommodated creep mechanism, while the microstructures observed in samples deformed to higher strain are compatible with structures observed following diffusional creep. In samples deformed to lower strain, elongated olivine and pyroxene grains aligned sub-parallel to the shear direction, and dynamically recrystallized grains formed in both phases. In contrast, in samples deformed to higher strains, mixtures of small, rounded grains of olivine and pyroxene were developed. The mechanical and microstructural evolution observed in this study are an important step toward understanding dynamic processes of strain localization and rheological weakening during plastic deformation of the lithosphere necessary for the initiation and persistence of plate tectonics.

Keywords: phase mixing , olivine and orthopyroxene aggregates

Temperature dependence of polycrystal anelasticity at near-solidus temperatures: toward clarification of the underlying mechanism and applications to seismology

*Hatsuki Yamauchi¹, Yasuko Takei¹

1. Earthquake Research Institute, The University of Tokyo

For a quantitative interpretation of seismic structures, it is needed to assess the effects of temperature, melt fraction, and grain size on the rock anelasticity. However, due to the limited understanding on the underlying mechanism, it is difficult to apply the experimental data to the condition of the mantle. To address this lack, we performed forced oscillation tests on the rock analogue (polycrystalline aggregates of organic "borneol") and measured modulus and attenuation over a wide frequency range.

Attenuation spectra obtained from polycrystalline materials are generally represented by the superposition of a monotonic "background" and a broad "peak" which exists at relatively high frequencies. The background, which has been observed robustly in all experiments, follows the Maxwell frequency ($f_M = M_0/\eta$, M_0 = unrelaxed modulus, η = diffusion creep viscosity) scaling. This shows that the mechanism of the background is "diffusionally accommodated grain boundary sliding," which is rate-limited by matter diffusion in the same manner as the diffusion creep. Although we have a general consensus about the scaling law and mechanism of the background, those for the peak are still controversial. It is crucial to better understand the peak, because it dominates the background at seismic frequencies.

We focus on the relationship between peak and partial melting, such that a large peak is obtained for melt-bearing rocks. Recent data obtained from the analogue samples show that even at subsolidus temperatures the amplitude and width of the peak increase with increasing T/T_m (T_m : solidus temperature) [Takei et al., 2014]. This result suggests that, even without melt, low Q and low V can occur at near-solidus temperatures. However, their data are limited to $T/T_m < 0.93$. In order to understand the effect of partial melting on the peak, it is important to investigate anelasticity at both subsolidus and supersolidus temperatures.

We measured anelasticity of the rock analogue at near-solidus temperatures ranging from subsolidus to supersolidus temperatures ($0.88 < T/T_m < 1.01$). In addition to the forced oscillation tests at 2×10^{-4} Hz $< f < 100$ Hz, we performed the ultrasonic test to measure the unrelaxed modulus and the creep test to measure the diffusion creep viscosity to calculate f_M . Also, from the reduction of the ultrasonic velocity by partial melting, we estimated the total relaxation strength which exists at higher frequencies than the ultrasonic frequency (> 700 kHz). The results are as follows. (1) Although the total relaxation strength of the background is constant regardless of various experimental conditions, that of the peak increases with increasing T/T_m , showing the breakdown of the Maxwell frequency scaling in the peak. (2) The increase of the total relaxation strength of the peak starts at the subsolidus temperature ($T/T_m = 0.93$), indicating that the mechanism of the peak is some solid-state mechanism. This result is also supported by the ultrasonic data which show that the relaxation by the melt squirt flow mechanism occurs at much higher frequencies than the peak (> 700 kHz). (3) Samples which experienced partial melting sometimes show a hysteresis such that the large peak observed in the partially molten state remains even below the solidus temperature. This implies that even after the solidification a connected network of grain-edge tubules works as a fast diffusion path and enhances the peak. These results provide a key to clarify the mechanism of the peak. We further discuss the implications to seismology.

Keywords: anelasticity, seismic wave velocity and attenuation, partial melting

Effect of Dislocations on Rock Anelasticity: Experimental Approach by Using an Analogue Material

*Yuto Sasaki¹, Yasuko Takei¹, Christine McCarthy², Ayako Suzuki¹

1.Earthquake Research Institute, University of Tokyo, 2.Lamont-Doherty Earth Observatory, Columbia University

Rock anelasticity causes seismic wave dispersion and attenuation. Therefore, it is important to understand the mechanism of anelasticity to know about the Earth's interiors from seismic tomographic images. Grain boundary sliding and dislocation motion have been two major mechanisms proposed for the rock anelasticity. Although extensive studies on the grain boundary sliding have been performed [1-4], few experimental studies have been performed on the effect of dislocations on the rock anelasticity [5, 6]. In this study, by using the organic polycrystalline material (borneol $C_{10}H_{18}O$, melting temperature $T_m=204^\circ\text{C}$) as a rock analogue [3], the effect of dislocations on anelasticity was measured accurately over a broad frequency range (10^2 - 10^4 Hz).

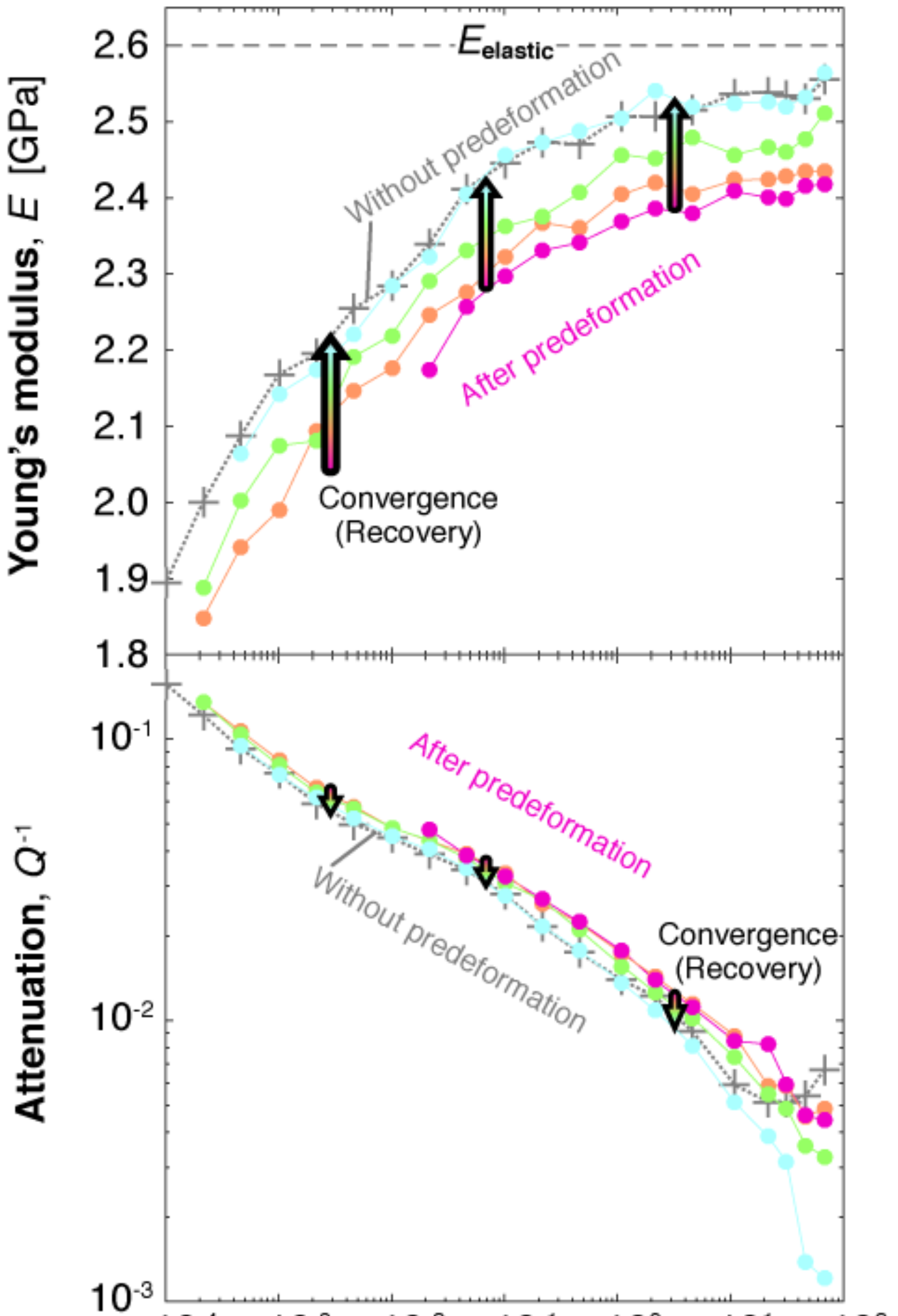
First, in order to know the flow law of this analogue material, uniaxial creep tests were performed at $T/T_m=0.66$ ($T=40^\circ\text{C}$) and 0.68 ($T=50^\circ\text{C}$) and at various differential stresses from $\Delta\sigma=0.27$ to 2.3 MPa. To avoid the occurrence of cataclastic flow, confining pressure $P_c=0.8$ MPa was applied in a pressure vessel with a frictionless uniaxial piston designed by T. Sato in soil mechanics. As a result, we captured a transition from a linear ($n=1$) creep to a power law ($n=5$) creep: the transition occurs at $\Delta\sigma\approx 1.4$ MPa for $T/T_m=0.68$ (50°C) and at a higher $\Delta\sigma$ for $T/T_m=0.66$ (40°C). In the deformed sample ($\Delta\varepsilon\sim 0.5$), grain boundaries became wavy and the grain size showed a larger variation than the undeformed samples, indicating the occurrence of grain boundary migration associated with dislocations. Therefore, we considered the power law creep as dislocation creep which introduced dislocations into the samples.

Next, three creep tests with $\Delta\sigma=0.27$ (diffusion creep regime), 1.4 (transitional regime), 2.1 MPa (dislocation creep regime) were conducted on the same sample in the increasing order, and after each creep test anelasticity of this sample was measured repeatedly to detect the effect of predeformation and also to detect a temporal evolution during the anelasticity measurements. Each predeformation was performed in the pressure vessel at $P_c=0.8$ MPa and $T/T_m=0.68$, and the deformed sample was cooled down to room temperature under the differential stress. The predeformation took about 16-23 hours and the cool down took about 6 hours. The sample was then removed from the vessel and anelasticity was measured in the forced oscillation apparatus [3] at ambient pressure: Young's modulus E and attenuation Q^{-1} were measured over a broad range of frequencies $f=10^2$ - 10^4 Hz and at several temperatures from $T/T_m=0.59$ (10°C) to 0.66 (40°C). The results can be summarized as follows. (1) The anelasticity obtained after the test with $\Delta\sigma=0.27$ MPa and $\Delta\varepsilon=0.007$ agreed well with the previous result measured under the offset stress $\Delta\sigma=0.27$ MPa [3]. (2) In contrast, after each of the latter two tests ($\Delta\sigma=0.14$ MPa and $\Delta\varepsilon=0.036$, $\Delta\sigma=2.1$ MPa and $\Delta\varepsilon=0.12$, respectively), Young's modulus E was lower and attenuation Q^{-1} was higher than the results in (1), and these changes were larger for the larger stress. (3) Over time, E and Q^{-1} gradually increased and decreased, respectively, finally converging into the property measured in (1). These results are considered to be attributable to the dislocations and their recovery.

[1] Morris and Jackson, 2009, *J. Mech. Phys. Solids*

- [2] Jackson *et al.*, 2014, *PEPI*
- [3] Takei *et al.*, 2014, *JGR*
- [4] Gribb and Cooper, 1998, *JGR*
- [5] Guéguen *et al.*, 1989, *PEPI*
- [6] Farla *et al.*, 2012, *Science*

Keywords: anelasticity, dislocation, seismic attenuation, analog experiment, polycrystal, defect



Fabric transition in olivine due to temperature and stress at high pressures

*Ayako Suzuki^{1,2}, Shenghua Mei¹, David L Kohlstedt¹, William B Durham³, Nathaniel A Dixon³

1.University of Minnesota, 2.Earthquake Research Institute, University of Tokyo, 3.Massachusetts Institute of Technology

The crystallographic fabric induced by deformation of mantle rocks reflects the dominant dislocation slip system and results in both rheological and seismic anisotropy in the upper mantle. The strength of the individual slip systems in olivine single crystals and the development of crystallographic fabric in olivine aggregates have been studied experimentally mainly in the high-temperature creep regime, with few measurements in the low-temperature plasticity regime. While a climb-controlled mechanism is important at higher temperatures and lower stresses, the dislocation slip mechanism in the low-temperature plasticity regime is considered to be glide-controlled. At low temperatures and high stresses, deformation of olivine aggregates follows an exponential flow law because dislocation motion requires a stress-dependent activation enthalpy for overcoming the Peierls barrier. In order to understand deformation mechanism and the dominant slip systems in the low-temperature plasticity regime, we investigated fabric evolution in olivine aggregates deformed experimentally at different temperatures changing from low to high at high pressures.

Samples were polycrystalline aggregates of San Carlos olivine with a grain size of 5-10 μm . Deformation experiments were carried out using the D-DIA apparatus at X-ray beamline X17B2 in the National Synchrotron Light Source (NSLS), Brookhaven National Laboratory. Samples were deformed to strains of 20-30% at a constant displacement rate of $0.1\text{-}6.8 \times 10^{-5}$ /s, temperatures of 673-1573 K, pressures of 4-9 GPa, and differential stresses of 0.6-3.8 GPa. Creep data at the highest temperature ($T = 1573$ K) and lowest stress indicated a dislocation, power-law creep mechanism, while creep results at lower temperatures ($T < 1273$ K) and higher stresses revealed an exponential flow mechanism (Mei et al., 2010).

After deformation experiments, we determined the crystallographic fabric (CPO, crystallographic preferred orientation) in the deformed samples using electron backscattered diffraction (EBSD). At the highest temperature ($T = 1573\text{K}$) and lower stresses ($\sigma < 1$ GPa), the poles of the (010) planes concentrated parallel to the maximum principal stress. This concentration of (010) planes is more dispersed at a temperature of 1473 K. In contrast, at lower temperatures ($T < 1373$ K) and higher stresses ($\sigma > 2$ GPa), the poles of the (100) planes concentrated parallel to the maximum principal stress. The change of crystallographic fabric in deformed samples is roughly consistent with the change of deformation mechanisms based on the analyses of mechanical data as stated above. This transition in slip plane associated with a change in temperature and stress is consistent with a difference in dominant slip systems of (010)[100] at higher temperatures and low stresses and (100)[001] at lower temperatures (Bai et al., 1991; Durham and Goetze, 1977; Tielke, 2016), indicating that the dominant slip system in the glide-controlled low-temperature plasticity regime differs from that in the high-temperature climb-controlled creep regime.

Keywords: low-temperature plasticity, slip system, olivine

Lattice-preferred-orientation of hcp metals studied by high-pressure deformation experiments

*Yu Nishihara¹, Tomohiro Ohuchi¹, Takaaki Kawazoe², Genta Maruyama¹, Yusuke Seto⁴, Yuji Higo⁵, Ken-ichi Funakoshi³, Yoshinori Tange⁵

1.Geodynamics Research Center Ehime University, 2.Bayreuth Geoinstitut, 3.CROSS, 4.Kobe University, 5.JASRI

Many hypotheses have been proposed for origin of seismic anisotropy in the Earth's inner core which consists of solid metal (e.g. Sumita and Bergmann, 2009). Plastic deformation of constituent material (most probably hexagonal-close-packed (hcp) iron) is one of the candidate processes to form the inner core anisotropy. Thus knowledge of deformation-induced lattice preferred orientation (LPO) of hcp-iron is important for understanding of nature of the inner core. In this study, we have carried out shear deformation experiments on hcp-iron and its analogue materials, hcp-Co and hcp-Zn, and determined its deformation induced LPO.

Shear deformation experiments were carried out using a deformation-DIA apparatus at high-pressure and high-temperature. Experimental conditions were 14–18 GPa and 723 K for Fe, 3 GPa and 673 K for Co, and 2 GPa and 573 K for Zn. Development of LPO in the deforming sample was observed in-situ based on two-dimensional X-ray diffraction using an imaging plate or X-ray CCD detector and monochromatized synchrotron X-ray. In shear deformation of Fe, $\langle 0001 \rangle$ and $\langle 112(_)0 \rangle$ axes gradually aligned to be sub-parallel to shear plane normal and shear direction, respectively, from the initial random orientation. In final LPO of Fe, $\langle 0001 \rangle$ and $\langle 112(_)0 \rangle$ axes are back-rotated from shear direction by $\sim 30^\circ$. On the other hand, in the deformation experiments of Co and Zn, the $\langle 0001 \rangle$ was aligned to parallel to shear plane normal. The above results suggest basal slip $\langle 112(_)0 \rangle \{0001\}$ is the dominant slip system in these hcp metals under the studied deformation conditions. The deviation of LPO of Fe from ideal orientation is presumably due to friction on the bottom plane of piston under higher pressure conditions.

It has been shown that Earth's inner core has an axisymmetric anisotropy with P-wave traveling $\sim 3\%$ faster along polar paths than along equatorial directions. Although elastic anisotropy of hcp-iron at the inner core conditions is still controversial, recent theoretical studies consistently shows that P-wave velocity of hcp-iron is fastest along $\langle 0001 \rangle$ direction at least at low-temperatures. Our experimental results could be suggesting that most part of the inner core deforms with shear plane sub-parallel to equatorial plane.

Keywords: hexagonal-close-packed metal, lattice preferred orientation, inner core

The mechanical property of a tunnel structure in wet granular layer

*Ayuko Shinoda¹, Shin-ichi Fujiwara², Hiroaki Katsuragi¹

1.Graduate School of Environmental Studies, Nagoya University, 2.Museum, Nagoya University

Stable burrows in wet sediments dug by tidal and shore animals play important roles not only in the ecological behaviors of the animals, but also in material circulation in the substrate and the sediment conditions. Thus, the burrow stability problem has been a challenging topic in the fields of sedimentology and biology. Modern ocypodid crabs are known to dig deep burrows in a sandy beach (Seike and Nara, *Palaeogeog., Palaeoclimat., Palaeoecol.*, 252 (2007) 458). However, it has not been clarified that how stable these burrow structures are against the external loading.

For the quantitative understanding of strength of a burrow in sandy beach, we modeled it by a tunnel structure in wet granular layer, and focused on mechanical property of wet granular matter. According to the previous works, tensile strength of wet granular column nonlinearly depends on liquid content (Scheel et al., *Journal of Physics: Condensed Matter*, 20 (2008) 494236, Herminghaus, *Wet Granular Matter: A Truly Complex Fluid*, World Scientific (2013)). The origin of this nonlinear response of wet granular matter to external loading has not yet been revealed sufficiently.

Moreover, little is known about the strength of a tunnel structure formed in wet granular layer. In this study, we conducted a simple experiment to investigate the mechanical property of a tunnel structure in wet granular layer. In the experiment, we observed how the tunnel structure deformed when it was uniformly loaded from the top of the layer with a very slow loading rate. By taking and analyzing the movies of deforming tunnel structures, we examined the temporal evolution of a projected cross section of the tunnel structure. Furthermore, based on the discussion of stability of tunnels in the soil (Knappett and Craig, *Craigs Soil Mechanics*, Spon Press (2012)), we estimated the maximum shear stress applied to the tunnel structure at each state. The experimental result showed that the mode of deformation depends on both liquid content and packing fraction.

Particularly, the liquid-content dependence of the mechanical response is not monotonic. In addition, we defined two types of strengths characterizing a tunnel structure: yield and maximum stresses. As a result, we found that these strengths strongly depend on packing fraction. Besides, they show qualitatively different liquid-content dependence in relatively high liquid content regime. Finally, we briefly discussed a possible application of the experimental result for estimating the upper limit size of tunnel structure in a sandy beach environment by using the experimental result and information obtained in previous works (Seike, *Marine Biology*, 153, (2007) 1199-1206, Sassa and Watabe, *Report of the Port and Airport Research Institute*, 45, 4,(2006) 61-107).

Feasibility Study of Morphological Characterization to Comminuted Particles by A Particle Characterization Approach (2)

*Daisuke Sasakura¹, Osamu Kuwano²

1.Malvern Japan ,Div of Spectris Co.Ltd,., 2.JAMSTEC

A faults zone contains fine rock powders called gouge that have been ground up by past fault motions.

Particle size distribution and particle shape of gouge particles may affect the frictional properties of the fault and reflect the comminution process by the past fault motions.

It is well known that particle size distribution (PSD) of fault gouge show power-law distributions. Exponent of this power law is considered to reflect the style and degree of deformation.

In this report, we will discuss about the relationship between the particle morphology and a style and a degree of comminution of model particles by automated particle image analysis and laser diffraction as a particle characterization method.

We did several shear experiments using a rotary shear apparatus with the shear displacement ranges between 10mm to 10m.

As an automated particle image analysis, Morphologi G3-SE (Malvern Instruments) was used for evaluation of particle size and shape.

The observation mode was diascopic mode (Transmittance mode) and a magnification was choose to sufficient to cover 1 to 1,000um.

The sample was dispersed with SDU (Sample Dispersion Unit) which attached Morphologi G3-SE.

Number of measured particles was over than ten thousand and a parameter filter function on software was used based on shape and pixel number of particle image.

We also used a laser diffraction instruments with dry dispersion methods, Mastersizer3000 with Aero unit (Malvern Instruments) for evaluation of particle size in less than 1um as fine particles.

Keywords: Fault gouge, Particle size, Particle Shape, Commutation, Fractal Distributions

Large Scale High Precision Sand Box Experiments:
Precise Measurements of Precursory Signal Preceding to Frontal Thrust Formation

*Osamu Kuwano¹, Takane Hori¹, Hide Sakaguchi¹, Daisuke Nishiura¹, Mikito Furuichi¹, Miki Yamamoto¹, Yasuhiro Yamada¹

1. Japan Agency for Marine-Earth Science and Technology

In order to find out the mechanism of the three-dimensional complex shape formation in sequential thrust and uplift of an accretion prism, we have developed a large-scale high precision sandbox experimental apparatus since 2011. After a number of modifications in the experimental apparatus and experimental procedure, we developed a prototype of the apparatus in 2014. In specimen preparation, the thickness of a sand layer is controlled with the precision of less than single particle size.

As a result, we obtained high reproducibility of the thrust formation including its position. With such a well-controlled experimental system, we found the precursory signal prior to thrust formation. In order to grab and understand the signal, we further improved the apparatus by installing the laser displacement sensor (resolution 0.1 μ m, span 800mm), a force sensor, and camera array for surface measurement. We will report the detailed information on the experimental apparatus our new findings.

Keywords: precursor, earthquake, sandbox experiment

Liquefaction experiments with a low permeability upper layer : dependence on layer thicknesses

*Moe Mizuno¹, Ikuro Sumita¹

1. Graduate school of Natural Science and Technology, Kanazawa University

When a water-immersed granular layer is shaken strongly enough by an earthquake, liquefaction occurs. If this layer consists of a low permeability upper layer, flame structures form and sand boils are observed. Previous liquefaction experiments have shown that when such layers are shaken the number and the area of sand boils decrease as the ratio of the thicknesses of the upper to lower layer increases (Yamaguchi et al. 2008). However no physical interpretation of these results have been made, and the effect of each layer thickness has not been clarified. Here we conduct a series of experiments with a range of combinations of the two layer thicknesses to quantitatively study how liquefaction and related phenomena depend on the thickness of each layers.

We use a small case filled with a mixture of glass beads and water. The glass beads are size graded such that the upper layers consist of fine particles with a diameter of 0.05 mm and the lower layer consists of coarse particles with a diameter of 0.22 mm. As a result the upper layer is 32 times less permeable compared to the lower layer. We vary the thicknesses of each layer in the range of 0 to 40 mm. The cell is shaken vertically for 5 s at an acceleration of 30 m/s² and a frequency of 100 Hz. We use a high-speed camera and record the images which are then analyzed in detail. From a series of experiments we recognize three phenomena, the compaction of the whole layer, formation of the flame structure, and eruption of water and glass beads. These phenomena are the consequence of gravitational (Rayleigh-Taylor) instability at the two-layer boundary (Yasuda & Sumita, 2014, 2016). Compaction occurred in all experiments whereas the formation of the flame structure or eruption water and glass beads occurred only when the upper layer is sufficiently thin. We studied the upper layer thickness dependence in detail for the case in which the lower layer thickness is in the range of 22-26 mm. We find that the wavelength of flame structure increases and the growth rate decreases as the upper layer becomes thicker. It appears that there is an upper limit wavelength. We also find that the peak amplitude becomes largest when the upper layer is at an intermediate thickness. We classified the results of all experiments using the values of the growth rate of the instability. We find that when the lower layer is thin, the growth rate depends on both the upper and lower layer thickness. However when the lower layer becomes thicker it depends on mainly on the upper layer thickness.

Our experimental results can be understood as follows. From Coulomb's law of friction, the interparticle friction increases with depth z as $\sigma = \mu \Delta \rho \Phi g z \dots (1)$, where μ is the coefficient of friction, $\Delta \rho$ is the particle-water density difference, Φ is the packing fraction, g is the gravitational acceleration. As a result, we estimate that when the z is greater than a critical, friction exceeds inertia, and fluidization does not occur at the two-layer boundary. Linear stability analyses for viscous fluids (Whitehead & Luther, 1975) indicate that the wavelength λ and growth rate p of the instability can be expressed as $\lambda \propto \varepsilon^{1/3} h \dots (2)$, $p \propto \varepsilon^{-2/3} h \dots (3)$, where ε is the upper to lower layer viscosity ratio and h is the thickness of the fluidized layer beneath the two-layer boundary. It follows that our result can be interpreted as a consequence of increasing ε with the thickness of the upper layer. Substituting the measured λ and p into Eq.(2),(3), we estimate that ε increased from 3 to 495 as the upper layer become thicker. This result is consistent with the increase of friction at the 2-layer boundary according to the Eq.(1). We consider that our results of upper layer thickness dependence can be interpreted as a result of the increase of effective viscosity of the upper layer.

Keywords: Liquefaction, earthquakes, low-permeability layer, gravitational instability, thickness dependence

Energetic Assessment of Frictional Instability and Quantitative Evaluation of Microstructural Development with Shear

*Momoko Hirata¹, Jun Muto¹, Hiroyuki Nagahama¹

1.Dept. Earth Science, Tohoku Univ.

1. Introduction

Frictional instability has been evaluated empirically by using a frictional parameter (velocity dependence) on the basis of the rate and state dependent friction law (Dieterich, 1979; Ruina, 1983). In addition, shear development in a gouge layer influences frictional instability (e.g., Byerlee et al., 1978; Logan et al., 1979; Ikari et al., 2011; Onuma et al., 2011). Ikari et al. (2011) pointed out a possibility that velocity dependence of friction changes with shear. However, it is difficult to accurately observe shear structures developed in recovered gouge samples and deal with shear zone development in gouge statistically. Therefore, the underlying theoretical relation between frictional instability and shear development has not been clear yet. In the present study, we aim to clarify (1) relation between frictional instability and shear development by energetic analysis, and (2) process of shear development toward frictional instability of gouge through theoretical and experimental analysis.

2. The energetic criterion for frictional instability

Deformation of particles progresses in an energetically efficient way (Rowe, 1962). Thus, both energy ratio defined as a ratio of input mechanical energy to output energy, and hence dissipation energy of particles become minimum. Stability of a mechanical system is influenced by energy. If a frictional system represented by a spring-slider model experiences frictional damping, the stored energy in the system decreases leading to stable slip. In contrast, if the system experiences negative frictional damping, the stored energy increases leading to unstable slip. Negative frictional damping indicates that friction force works to the direction of motion and might be related to shear development. Because the stored energy coincides with the difference in energy during deformation, the stored energy can be represented by the energy ratio between input energy to output energy through deformation. Thus, the energetic criterion for frictional instability is obtained from the relation between the stored energy and mechanical behavior of the frictional system.

3. The friction experiments

We analyzed data of friction experiments using simulated fault gouge (Hirata et al., 2014) to obtain energy ratio of gouge during friction experiments in gas apparatus. The cylindrical samples with dry quartz powder as gouge were loaded under 140, 160, and 180 MPa of confining pressures. Data about stress and strain in major and minor principal axes were recorded through strain gauges placed onto samples. The values of energy ratios of gouge were obtained based on these values.

4. Results and discussion

We clarified that the output energy has a linear relationship with input mechanical energy, but energy ratios changed slightly with shear. Change in the energy ratio which is a function of internal friction angles implies shear development. R1-shear angles from major principal stress axis can be estimated using internal friction angles (Morgenstern and Tchalenko, 1967). Thus, the energy ratio controlled by the internal friction angle closely related to shear development. R1-shear angles we estimated show that R1-shears becomes more parallel to a rock-gouge boundary before the occurrence of unstable slip. At 140 MPa of confining pressure, R1-shear was inferred to be developed almost parallel to the boundary (3 degrees to the boundary) at the top of a sample as deformation proceeds. The reduction of shear angles with respect to shear zone boundary with

progressive shear is consistent with previous works (e.g., Gu and Wong, 1994).

5. Summary

We investigated relation between frictional instability and shear development energetically. Our results revealed that (1) the energetic background for their relation; (2) the efficacy of the energetic criterion for frictional instability; and (3) shear development in gouge in situ.

Keywords: frictional instability, Rowe's theory, microstructural development, simulated fault gouge, friction experiments, energetic assessment

Distributions of physical property and anisotropy of unconsolidated sediments off Costa Rica under differential stress

*Saki Higa¹, Yoshitaka Hashimoto¹

1.Kochi University

Static moduli of rock are used in borehole stability to evaluate elevated pore pressure and tectonic stress distribution. The static and dynamic moduli of the same rock may significantly differ from each other. The main reason is likely to be the difference in the size of strain between the dynamic and static tests. In the dynamic properties the strain is about 10^{-7} , while static strain may be about 10^{-2} .

The purpose of this study is to reveal the relationship between static and dynamic moduli of unconsolidated sediments obtained from off Costa Rica, and to evaluate anisotropy of static moduli using shear strain. To achieve this purpose, we obtained (1) static Vp/Vs using volumetric strain and shear strain from experiments in differential stress, and (2) dynamic Vp/Vs from dynamic wave propagation experiments. Then Poisson's ratio was calculated using Vp/Vs. Using Poisson's ratio, static and dynamic Young's moduli were transformed.

Used materials are unconsolidated sediments obtained by IODP expedition 344. We focused on reference site U1414, frontal prism U1412, mid-slope U1380. Materials were remodeled into cylinder shape for the experiments.

Equipment of laboratory experiment consists of pressure vessel, three syringe pumps, computer, transducer, oscilloscope, displacement gauge. In laboratory experiment, pore fluid pressure was kept 1MPa. Effective pressure was controlled by changing axial pressure and confining pressure. We calculated in-situ effective pressure using sample depth, bulk density and assumption of hydrostatic pressure of pore pressure. We conducted 4-5 steps of experiment with isotropic pressure up to in-situ effective pressure. Between each isotropic condition, differential stress experiments were conducted. In differential stress experiments, axial pressure was increased and radial pressure was kept in constant; increment of differential stress is three times as large as increment of effective pressure. Axial strain was calculated from a value of axial displacement gauge. Volumetric strain and porosity were calculated from remaining volume of pore fluid pressure in a pump. When strain reached at equilibrium condition, waveform, a value of axial displacement gauge and remaining volume of pore fluid pressure were recorded.

In the results, static Vp/Vs ranges 1.5-1.6, and dynamic Vp/Vs covers 2.0-2.1. Using each Vp/Vs, Poisson's ratio, static and dynamic Young's moduli were calculated. The ratio of dynamic to static Young's moduli (K) was about 0.6. Dynamic physical properties can transform into static physical properties using K value. Dynamic S-wave velocity was about 25% slower than static S-wave velocity systematically in all samples.

Shear strain of samples from U1414 was larger than that of samples from sites U1412 and U1380. Shear strain is described by the difference between axial strain and radial strain, suggesting anisotropy in reference site is larger than that in wedge.

Keywords: static moduli, Costa Rica, unconsolidated sediments

Plasticity index and mechanical bifurcation of soils and rocks

*Naoto Kaneko¹, Jun Muto¹, Hiroyuki Nagahama¹

1.Department of Earth Science, Graduate School of Science, Tohoku University

In the field of soil mechanics, triaxial compression test is widely used to investigate mechanical properties of soils. Yielded specimens characterized by Mohr's stress circles have various deformation patterns depending on loading stages and stress ratios in spite of the same ground materials. Failure patterns of ground materials bifurcationally change to diamond, bulge and a pair of oblique shear patterns. The symmetry of deformation patterns (e.g. shear band patterns) has been illuminated by bifurcation analysis of governing equation of soil mechanics based on Cam-clay model. On the other hand, plasticity index, an empirical parameter to characterize the range of water contents where the soil exhibits plastic property, is known to describe mechanical characteristics (e.g. compressibility) of soils. However, it is an unknown theoretical relationship between mechanical bifurcation controlling the evolution of deformation patterns and plasticity index. Also the theoretical relationships between the empirical laws of soil strength and plasticity index have not been clear yet. Hence, we show that plasticity index theoretically determines deformation patterns of soils by Cam-clay model, and we prove that the index closely affects the bifurcation formulas on the basis of Shibi and Kamei (2002)'s bifurcation analysis. From the view point of the plasticity index, deformation facies representing various deformation patterns of rocks in geologic condition are controlled by mean ductility and ductility contrast, as quantitatively proposed by Uemura (1981).

Keywords: plasticity index, deformation patterns, bifurcation

Analogue experiments for understanding of factors controlling morphological transition in columnar joints

*Ai Hamada¹, Atsushi Toramaru²

1. Department of Earth and Planetary Sciences, Graduate School of Sciences, Kyushu University,
2. Department of Earth and Planetary Sciences, Faculty of Sciences, Kyushu University

Columnar joints in lava flows and welded tuffs have two different types of column structures adjacently within a single flow unit in terms of columns widths, column configurations and the directions of developed columns, which are called as Colonnade and Entablature. Colonnade consists of relatively large width, straight and ordered columns, while Entablature consists of relatively small width, curved and disordered columns. Columnar joints are formed due to volume contraction during cooling. The isotherms at a time are assumed to be perpendicular to the direction of columns if the directions of maximum tensile stresses are parallel to the isotherms. The assumption, which is based on thermal diffusion process during cooling, has been applied to the formation of simple cases in the curved structures. However, it still has not clearly solved how the complex structure in Entablature is related to the complex isotherms. In order to understand the formation process of Colonnade structure in columnar joints, analogue experiments using starch and water mixture as analogue materials have been conducted in terms of morphology, theory and crack formation. However, attempts to reproduce morphological transition from Colonnade to Entablature have not been conducted yet. This thesis aims at understanding the factors to control the transition between Colonnade and Entablature by means of drying experiments as well as reproducing curved structures which are seen in Entablature. I investigated the process of crack propagations and the relations between the water distribution and crack developments in mixture by observing X-ray CT images with changing time. Three sets of experiments conducted focus on: (1) Transfer processes in drying and cracking samples, (2) Water concentration and the direction of cracks with time and (3) Effects of sudden increase in desiccation rate on drying and cracking processes. The samples after all experiments are observed by using X-ray CT and compared with the models based a diffusion equation in Experiment 1 and 2. Further morphological analysis is developed for images taken in Experiment 3 for suggesting the possibility of column nucleation in nature. Results suggest: 1. Water transportation within the mixture can be explained by the diffusion process, 2. Crack development occurs perpendicular to the iso-water concentration surface in the mixture and 3. Instantaneous increase in desiccation rate causes columns nucleation.

I propose a scenario of morphological transition from Colonnade to Entablature at Shakushiwa, which shows a threefold structure (Upper Colonnade -Entablature -Lower Colonnade) within Aso-4 welded tuffs in Oita prefecture, Japan, on the basis of above suggestions by introducing two heat transports: vertical heat transport within rocks by thermal diffusion to the uppermost of the rock, Q_1 and heat transport through the cracks, Q_2 . Central Entablature has radial structures by originated from the tips of cracks in Upper Colonnade. These radial structures are horizontally aligned repeatedly. As the cooling process proceeds in Upper Colonnade by thermal diffusion Q_1 from hotter interior of the rock to the cooling surface at the top of the rock, cracks develop perpendicular to the isotherm of T_c , which is the temperature when cracks restart to propagate to form Upper Colonnade. When cracks developed from Upper Colonnade part to the boundary to Entablature, cracks themselves become the cooling surface and the heat transport Q_2 proceeds. This cooling process makes the configuration of the isotherm T_c to be convex downward around the tips of cracks. The heat transport transition from Q_1 to Q_1+Q_2 causes the abrupt increase in cooling rate and form smaller widths of columns than those in Upper Colonnade by column nucleation. Such

morphological change of columns is consistent with the field observation.

Keywords: Columnar jointing, Morphological transition, Analogue experiment

Rheological law and viscous-brittle transition of 3 phase magma; a case study for the 1946 andesitic lava from Sakurajima volcano, Japan

*Hidemi Ishibashi¹, Takahiro Miwa², Yuta Mitsui¹

1.Faculty of Science, Shizuoka University, 2.NIED

Uniaxial compression deformation experiments were done for the 1946 andesitic lava from Sakurajima volcano, Japan, under conditions of temperatures from 1300 to 1130 K, strain rates from $10^{-2.5}$ to $10^{-5.5} \text{ s}^{-1}$, and ambient pressure. The starting lava sample has ca. 20 vol. % of bubbles and the solid part consists of ca. 47 vol.% of rhyolitic glass, ca. 23 vol.% of microlites and ca. 30 vol.% of phenocrysts of plagioclase, pyroxenes, and Fe-Ti oxides. The experiments were done by using the uniaxial deformation apparatus at ERI, University of Tokyo. Deformation experiments were done after ca. 2h pre-heating at the experimental temperatures and the samples were quenched to 873 K with 15 min after the deformation was finished. During the experiments, stress and sample high were monitored under constant temperature. Deformation rate was changed stepwise due to examine non-Newtonian behaviors. Viscosity was calculated by the equation of Gent (1960) from the monitored stress-sample high dataset.

The lava behaves as a power law shear-thinning fluid at temperatures from 1300 to 1160 K under the experimental strain rate conditions. Viscosity increases from ca. $10^{7.3}$ to ca. $10^{11.3} \text{ Pa s}$ with decreasing temperature and strain rate. An equation describing its dependence on temperature and strain rate was proposed. Relative viscosity, defined as the ratio of magma viscosity/melt viscosity, is almost constant around 100 (with assumption that melt water content is 0.2 wt. %) regardless of experimental temperature. At 1130K, fracturing occurs at strain rate of $10^{-3.5} \text{ s}^{-1}$ whereas the lava behaves as viscous under strain rate of 10^{-4} s^{-1} . Crystallinity is almost constant around 0.53 regardless of temperature.

Deborah numbers are calculated to be lower than $10^{-2.65}$ for non-fractured samples and ca. $10^{-2.65}$ for the fractured sample. The relation between crystallinity and critical Deborah number for viscous-brittle transition is consistent with the criteria for crystal-bearing magmas proposed by Cordonnier et al. (2012). Present results indicate that the critical stress for viscous-brittle transition is ca. $10^{7.4} \text{ Pa}$. The present rheological law was used to calculate flow velocity of the 1946 andesitic lava flow; the result calculated at 1273 K well explains the field observation of Hagiwara et al. (1946). The temperature is consistent with petrological constraints. The calculated maximum shear stress in the lava flow is lower than $10^{6.5} \text{ Pa}$, indicating that any process concentrating stress on the lava surface is required to form the blocky structure.

Keywords: Rheological law, Lava flow, brittle-viscous transition, magma, Sakurajima volcano

Strain Behavior and Deformation Property of Aji Granite under Triaxial Compression Tests

*Kazuki Sawayama¹, Ikuo Katayama²

1.Department of Earth Resources Engineering, Kyushu Univ., 2.Department of Earth and Planetary Systems Science, Hiroshima Univ.

Fracture behavior of rock has been much researched because it is related to the mechanism of the earthquake and strength of the earth's crust. Recently, outcomes of these researches have been applied for hydraulic fracturing, which can create artificial geothermal fluid reservoir and such resources may have potential to solve Japan's energy issues. However, this application (Hot Dry Rock power generation) has some problems and fundamental research is needed in order to understand deformational properties of crustal rocks. Therefore, we investigated the effects of confining pressure and pore pressure on the strain behavior and deformation properties of granite. We conducted strain measurements during triaxial compression tests of Aji granite at constant strain-rate ($1.7 \times 10^{-5} \text{ s}^{-1}$) under confining pressure ranging between 10 and 40 MPa, and pore pressure ranging between 10 and 30 MPa. The experimental results showed that the maximum stress and the onset of dilatancy increase with effective pressure but slightly decrease under wet condition. Young's modulus increases slightly with effective pressure, whereas Poisson's ratio is nearly constant in our experiments. Dilatancy that is related to the formation of micro-cracks during deformation is suppressed at high confining pressure, while dilatancy tends to be enhanced at low pore pressure, and hence high effective pressure, under wet condition. This indicates that the stress concentration related to the formation of micro-crack can be relaxed at high pore fluid pressure. Wet experiments have shown a rapid increase of water injection volume within the specimen at stress level of 96–97% maximum stress, which is probably attributed to the formation of micro-crack network. In addition, such increase of water injection volume became nearly constant at and after maximum stress, indicating that pore volume is may not be changed by localization of micro-cracking or macroscopic fracture. Based on these results, it is expected in hydraulic fracturing test that fracture under the ground can be efficiently created by lower injection rate and macroscopic fracture may occur soon after pore pressure decreases.

Keywords: Stress-strain relationship, Dilatancy, Pore pressure, Triaxial compression test, Granite, Hot Dry Rock power generation

Grain size distribution of quartz in the Sanbagawa metamorphic belt analyzed by the electron back-scattered diffraction (EBSD) method

*Tadamasa Ueda¹, Ichiko Shimizu¹

1. Department of Earth and Planetary Science, Graduate School of Science, The University of Tokyo

The size of dynamically recrystallized grains in naturally deformed rocks has been used for paleostress estimates. However, the meanings of the "average" grain size in previous piezometric studies (e.g. Stipp and Tullis, 2003) often have two large problems. One is derived from difficulty in distinguishing grains and subgrains under an optical microscope, and the other is unclarity about what is the appropriate definition of the "average" grain size (e.g., the arithmetic mean, the root mean square). Different definitions could yield different stress estimates.

We measured grain size of quartz by optical microscopy and electron back-scattered diffraction (EBSD) mapping. In the optical method, grain boundaries were manually traced on photomicrographs according to the difference in extinction angles and analyzed by an image processing software. In the EBSD analyses, the grain boundaries with the misorientation angles exceeding 12° were automatically detected based on the Euler angles of the crystal lattice orientation. EBSD mapping was conducted with changing step size, 0.5, 1, 2, and 8 microns. The size of each grain was defined as the diameter of the equivalent circle.

We analyzed microstructures of a quartz schist in the garnet zone of the Sanbagawa metamorphic belt, which was taken from the Asemi-gawa area, Shikoku Island, Japan. Under an optical microscope, large quartz grains show oblique shape fabric and intracrystalline deformation features, and small quartz grains are formed at the margins of large quartz grains.

The grain size distributions quantified by the optical analysis and EBSD showed severely right skewed shapes. Hence, different definitions of representative grain size yielded quite different values. The distributions are far different from the bell-shape distribution known for static grain growth. Right skewed distributions can be produced by a simple nucleation-and-growth model (Shimizu, 1999, *Phil. Mag.*). The modes of the distributions vary with methods and step sizes, ranging from ~10 to ~50 μm . Because the mode was not well defined, we used, as the representative value, the class of grain size occupying the largest area in each mapped area, which can be related to the length scale in the nucleation-and-growth model of Shimizu (1999) and is robust because it reflects measurements of large grains. In the result, this value ranges from 110 to 120 microns. Using a revised theoretical grain size piezometer (Shimizu and Ueda, 2016, *JpGU*), which takes temperature dependence into account, and the temperature estimate of the sampling locality (516.4° C; Bayssac et al., 2002), the differential stress is 29 and 62 MPa, assuming intracrystalline recrystallization and marginal recrystallization, respectively. These stresses are higher than that given by the empirical piezometer of Holyoke and Kronenberg (2010) (17 MPa), which uses the root mean square as the representative grain size and does not take the temperature effect into account. We will show results from quartz schists of other zones of the Sanbagawa metamorphic belt.

References:

- Holyoke C. W., Kronenberg A. K., 2010, *Tectonophysics*, v494, p17
Shimizu, I., 1999. A stochastic model of grain size distribution during dynamic recrystallization., *Philosophical Magazine* A79, 1217-1231.
Stipp M., Tullis J., 2003, *GRL*, v30, no.21, 2088

Keywords: quartz, recrystallized grain size piezometer, Sanbagawa metamorphic belt

Effect of water on rheology of plagioclase under high temperature and high pressure

*Masanori Kido¹, Jun Muto¹, Sanae Koizumi², Hiroyuki Nagahama¹

1.Department of Earth Science,Tohoku University, 2.Earthquake Research Institute,The University of Tokyo

1. Introduction

Rheological behaviors of rocks depend on pressures, temperatures and chemical environment. Particularly, water is known to play an important role in rheology of rocks in terms of physical and chemical aspects by previous experiments. Here, two ways of water effects are considered. Pore fluid pressure reduces the effective stress of rocks supported by mineral frame. Water also reduces the strength of plastic deformation of minerals by increasing concentration of lattice defects. Moreover, tomographic observations have shown that there are fluid-rich zones beneath active fault zones and strain concentration zones in the middle-lower crust (e.g., Nakajima et al., 2010). It is proposed that water affects crustal deformation and earthquake occurrence (e.g., Iio et al., 2009). However, the effect of water on rheology has not yet been revealed quantitatively for lower crustal materials under pressure conditions equivalent to the lower crust. Moreover, in most of previous studies, experiments were performed under two end-member cases: water saturated or anhydrous conditions. Thus, it has not been understood in the environment that water is gradually introduced into samples similar to natural lower crustal condition.

2. Deformation experiment

In this study, we performed deformation experiments on synthetic anorthite (An) aggregates using the Griggs-type solid medium deformation apparatus. We added 0.5 wt% water to samples and infiltrated under high temperature and high pressure. Times for infiltration of water into samples were changed to investigate the variation of deformation behaviors associated with diffusion of water. Strain rate stepping test was performed at a temperature of 900 °C and a confining pressure of 1.0 GPa. Strain rates were 1st: 10^{-5} , 2nd: $10^{-4.5}$ and 3rd: 10^{-5} s^{-1} . Constant strain rate tests were also performed at a strain rate of $10^{-5} / \text{s}$, temperature of 900 °C and confining pressures of 0.8 and 1.1 GPa. The experimental conditions in the present study were roughly equivalent to the environment of the middle-lower crustal fluid-rich zones. Thus, the present study is suitable for investigating the effect of water on plastic deformation in such zones.

3. Results

In all experiments, wet samples were weaker than an anhydrous sample. Strain weakening was observed in experiments at a strain rate of $10^{-5} / \text{s}$ at all confining pressure conditions. Strengths tended to decrease with infiltration time or strain magnitude. Photomicrographs after the experiments of wet An deformed under confining pressure of 1.0 GPa were taken. Almost no deformation was observed in the upper part of the sample, and deformation was concentrated in the lower part.

4. Discussion and implication

We compared the measured differential stresses with predicted values by the flow law for wet An obtained by low pressure experiments (~ 0.4 GPa, Rybacki et al., 2006). The estimated stress values were higher than the measured values in our experiments under similar conditions. Moreover, because recovered samples were deformed in their lower part intensively, actual strain rates might be higher and estimated stress values became higher for that part than those estimates. This implies that the chemical effect of water, such as fugacity, in higher pressure condition might be larger than those predicted by lower pressure experiments. Present study shows that measured differential stresses of hydrous samples tended to decrease with infiltration time or strain magnitude. It is assumed that plastic deformation is promoted by increase of water-related defects by water

diffusion into samples. The results of present study indicate that the strength of lower crust become lower than previous studies.

Keywords: plagioclase, deformation experiments, water fugacity, strength of the crust

Technical developments on acoustic emissions monitoring under the upper mantle conditions

*Tomohiro Ohuchi¹, Xinglin Lei², Yuji Higo³, Yoshinori Tange³, Tetsuo Irifune^{1,4}

1.Geodynamics Research Center, Ehime University, 2.National Institute of Advanced Industrial Science and Technology, 3.Japan Synchrotron Radiation Research Institute, 4.Earth-Life Science Institute, Tokyo Institute of Technology

The subduction zone produces a major fraction of the Earth's seismic activity. Intermediate-depth earthquakes within the subducting slab form a double seismic zone. The mechanisms of intermediate-depth (> 40 km depth) and deep-focus (> 300 km) earthquakes are fundamentally different from those of shallow (≤ 40 km) earthquakes. This is because the frictional strength of silicate rocks is proportional to the confining pressure and it exceeds the upper limit of the stress level in the upper mantle (< 600 MPa: Obata and Karato, 1995) at pressures higher than 1 GPa (~ 30 km depth). The causes of intermediate-depth and deep-focus earthquakes have been attributed to dehydration of hydrous minerals (e.g., Peacock, 2001) and anticrack faulting during the phase transformation of olivine (e.g., Green et al., 1992), respectively. To understand the mechanisms of failure of rocks under the upper mantle conditions, experimental techniques on acoustic emission (AE) monitoring have been adopted to multianvil apparatuses or Griggs apparatuses.

Green et al. (1992) conducted AE monitoring by using a Griggs apparatus combined with an AE sensor. Dobson et al. (2002, 2004) and Jung et al. (2006) adopted 2 or 4 AE sensors to a multianvil apparatus. However, the three-dimensional location of AE hypocentres have not been determined in the experiments because of not enough number of sensors used in the experiments, even though determination of the location of AE hypocenter is critical in the judgement of brittle failure of the sample surrounded by the solid pressure medium. De Ronde et al. (2007) adopted 8 AE sensors to a multianvil apparatus and they succeeded to determine the position of AE sources. Recently, Gasc et al. (2011) succeeded to develop an experimental setup that allows determining the position of AE source by using DIA-type multianvil apparatus combined with 6 AE sensors. Schubnel et al. (2013) adopted the experimental setup reported by Gasc et al. (2011) to a D-DIA apparatus installed at a synchrotron facility, and they succeeded to measure strain and stress of the sample and AE signals. We have developed an experimental setup that is optimized for the determination of the location of AE hypocentres in a synchrotron D-DIA apparatus.

Similar to Schubnel et al. (2013), we developed an AE monitoring system optimized for a D-DIA apparatus installed at BL04B1, SPring-8. One of big difference between previous systems and our system is the use of the MA 6-6 system (Nishiyama et al., 2008). In our system, the AE sensors were pasted to the backside of the second-stage anvils. Use of the second-stage anvil as a wave guide enables us to shorten the distance between the sample and the AE sensors, namely, attenuation of AE waveforms is reduced. Another advantage of our system is the large-volume cell assembly (sample diameter: 3mm; length: 4mm). Because the error on the hypocenter location is usually a couple of millimeter (e.g., Gasc et al., 2011), use of a sample having a large volume is critical when we judge whether a hypocenter locates inside of the sample or not. We succeeded to conduct experiments on AE monitoring during the deformation of olivine aggregates at pressures 1-3 GPa and temperatures 600-1100 degC. Pressure, stress, and strain were measured in situ by using x-ray diffraction patterns and radiographies. AEs were also recorded continuously on six sensors, and three-dimensional AE source location were determined. We will report some the details of experimental results, and we will consider further improvements on the system.

Keywords: acoustic emission, D-DIA, earthquake

Deformation experiments of ringwoodite at low temperature conditions

*Masahiro Imamura¹, Tomoaki Kubo¹, Takumi Kato¹, Takumi Kikegawa², Yuji Higo³, Yoshinori Tange³

1.Kyushu University, 2.Photon Factory, High Energy Accelerator Research Organization, 3.Japan Synchrotron Radiation Institute

Seismic tomography images that some subducting slabs horizontally stagnate near 660km discontinuity (e.g., Fukao and Obayashi, 2013). However, it has been difficult to explain the large deformation of deep slabs in mantle transition zone because the flow law of constituent minerals such as ringwoodite has not been determined yet. Low temperature plasticity (Peierls mechanism) could be a dominant deformation mechanism in cold subducting slab. In order to construct the flow law of ringwoodite in this deformation mechanism, we conducted deformation experiments of $(\text{Mg}_{0.9}, \text{Fe}_{0.1})\text{SiO}_4$ ringwoodite at low temperature conditions. Here, we report its preliminary results.

High-pressure deformation experiments were conducted at 9-13 GPa and 500°C in constant-strain rate mode by Deformation-DIA apparatus installed at NE7 and BL04B1 beamlines in synchrotron facilities of PF-AR and SPring-8, respectively. We synthesized a polycrystalline ringwoodite with height of 1.2 mm and diameter of 0.9 mm at 22 GPa and 1400°C for 180 min from a single crystalline San Carlos olivine using a Kawai-type multi-anvil apparatus in Kyushu University. This was recovered and used as a starting material for the deformation experiment. Differential stress and axial strain of ringwoodite samples were estimated from the distortion of Debye ring and radiography image using 50 keV monochromatic X-ray.

Although deformation experiments were performed outside the ringwoodite stability field, we did not observe the back transformation up to at least 500°C. The sample stress almost reached steady state at the strain of about 3%, and then slightly increased under strain up to ~20%, suggesting the strain hardening. The effect of pressure was negligible in our experimental condition. The flow stresses of ringwoodite obtained at 500°C were 2.6-5.1 GPa at the constant strain rates of $1.2-5.9 \times 10^{-5} \text{ s}^{-1}$, which is smaller than those obtained at room temperature in the previous study (Nishiyama et al., 2005). Preliminary analysis of the creep data indicates that the stress exponent is about 6. The relatively large stress exponent may suggest that ringwoodite was deformed in low-temperature plasticity regime although further experiments are needed to construct the quantitative flow law.